

Bentonite Homogenisation – Laboratory Study of Homogenisation Processes in Buffer and Backfill Materials in Repositories

Ann Dueck¹, Lennart Börgesson¹ and Reza Goudarzi¹

Abstract

Swelling and homogenisation of bentonite materials are important functions of the bentonite to guarantee the requirements of the buffer and backfill after full water saturation in deposition holes and tunnels in a radioactive waste repository. A study including a laboratory testing programme with tests in different scales and complexity and modelling of the tests is financed by SKB.

In this article some tests and test results from laboratory tests in different scales are described and analysed. The results have been used to evaluate parameters and models for modelling homogenisation as described in another article.

A large number of fundamental very well controlled small-scale tests with simple geometries and swelling in radial or axial direction have been made. They show that homogenisation and healing properties of the investigated bentonites are extremely good but also that we have considerable density differences left.

Larger scale tests with more complicated geometries have also been done. In one of the test types swelling and homogenisation in long tubes have been studied with the purpose to study the effect of friction for limiting homogenisation. The other test type simulates loss of bentonite in two medium scale laboratory tests where a bentonite block with two large cavities were left to homogenise. The results show that the cavity has been very well healed by the swelling bentonite but also that the dry density in the centre of the former cavity is clearly lower than the density at the unaffected parts.

Keywords: Bentonite, homogenisation, radioactive waste, swelling tests, dry density, swelling pressure, angle of friction.

¹ Clay Technology AB, Sweden

1. Introduction

1.1 Background

Swelling and homogenisation of bentonite materials are important functions of the bentonite to guarantee the requirements of the buffer and backfill after full water saturation in deposition holes and tunnels in a repository. It is important to understand and be able to predict the final condition of the buffer after the swelling and homogenisation, which occurs both during the initial saturation and homogenisation of the buffer, which according to the KBS-3 concept consists of blocks and pellets, and also after possible loss of bentonite caused by for example erosion.

To increase the knowledge of the homogenisation process SKB has initiated and financed a homogenisation project that has been running during several years. The project consists of several parts; theoretical studies and modelling, fundamental laboratory swelling tests, laboratory study of the influence of friction, medium scale tests of a scenario involving loss of bentonite and long tubes tests with large density gradients.

The first laboratory tests series started in 2008 and in 2016 most test series were completed. The test results referred to in this report have been presented in several reports (Dueck et al [1, 2, 3, 4]). Compilations and analyses of the tests and results have been reported by Dueck et al [5].

Material models have been developed and verified with some of the laboratory test results from this project. These are also described by Dueck et al [5] and in another article by Börgesson et al [6].

1.2 Purpose

The main objective of the laboratory tests made in this project is to improve the understanding of homogenisation processes and to provide results that can be used for modelling some well-defined benchmark tests in order to improve the hydro-mechanical models of bentonite materials.

1.3 The homogenisation project

How well the bentonite self-seals and homogenises is investigated in the homogenisation project. The laboratory tests have mainly been made on specimens that have been water saturated or close to water saturated from start, which means that the saturation process has not been included in the tests.

The purposes of the project and the tests have been to

- understand how homogenisation evolves and ends,
- investigate the different factors influencing homogenisation,
- understand how much remaining inhomogeneities that may prevail in bentonite,
- be a base for creating hydro-mechanical models for the homogenisation process,
- evaluate model parameters,

- confirm the models and calculation tools by modelling different homogenisation cases.

The laboratory tests made in this project have been divided into four parts

- fundamental swelling tests to increase the knowledge about material parameters,
- measurement of friction between bentonite and other surfaces,
- homogenisation in long tubes where the effect of time also can be studied,
- homogenisation after loss of bentonite in the self-healing tests.

The modelling related to the laboratory test results from this project has included comparison with measured results and has mainly been concentrated on

- evaluation of models and model parameters and verification of the models by modelling the fundamental swelling tests,
- analyses and modelling of one test from the series with long tubes,
- modelling of one of the self-healing tests,
- development of a new hydro-mechanical model for COMSOL.

1.4 Laboratory test program

In this article a description of each test type is given together with important results and observations in the fundamental laboratory tests, the friction tests and the larger scale homogenisation tests.

The main results from the different test types consist of measured stresses during the tests and final distributions of density and water content determined on the specimens after dismantling.

The materials used for the tests have been the bentonites MX-80 (Wyoming bentonite from American Colloid Company) and Calcigel (Bavarian bentonite from Süd-Chemie AG) further described by Karnland et al [7] or Svensson et al [8]. The water supply during saturation and homogenisation consisted of de-ionized water or water with a low salt content.

2. Fundamental swelling tests

The fundamental swelling of water saturated bentonite specimens with access to water has been studied in mainly three different test series. The principles are illustrated in Figure 1.

- Axial swelling in a device with constant radius and limited height and with variation of the height of the gap.
- Radial swelling of the outer surface in a device with constant height and limited radius and with variation of the radial gap.
- Radial swelling into a cylindrical cavity in a device with constant height and radius and with variation of the radius of the cavity.

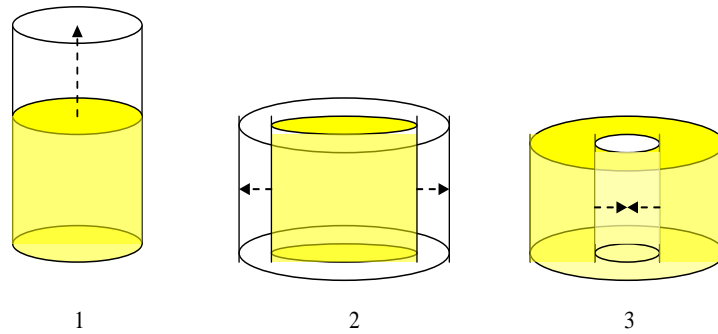


Figure 1: Illustration of the geometry of the three test types

Tests of this type have been run in two series: the basic-series and the so-called HR-series (High Resolution). In the basic-series small specimens with the height 20-40 mm and the diameter 50 mm were used which were saturated in the test device before the subsequent swelling. To improve this test type and to increase the resolution of the results, the HR-series were run with dimensions of the specimens doubled compared to the basic series, i.e. the height was 40 - 80 mm and the diameter 100 mm. The specimens used in the HR-series were basically water saturated at start and no saturation took place in the test device before the swelling. The number of tests of each type are given in Table 1 where the swelling s is calculated from the initial dry density ρ_{di} and the final dry density ρ_{df} according to Equation 1.

$$s = \frac{\rho_{di}}{\rho_{df}} - 1 \quad (1)$$

Table 1: Number of tests of each type of the fundamental swelling tests in the Basic and HR-series.

Material	MX-80		Calcigel		Total	Swelling magnitude
	Basic-series	HR-series	Basic-series	HR-series		s (%)
Type of swelling						
Axial	7	4	2	3	16	0 - 46
Radial outward	10	1	2	2	15	3 - 45
Radial inward	6	1	2	1	10	3 - 110
Swelling in all directions		1			1	43

Some of the fundamental swelling tests have been modelled. The modelling results are described by Börjesson et al [6, 9].

Two example of test results on MX-80 will be shown here. An analysis of the results by comparing the measured stress-density relations with earlier models will also be done.

2.1 Axial swelling of MX-80 (HR-A1)

In this test the axial swelling of MX-80 was tested in the HR-equipment. Figure 2 shows the test set-up. The axial pressure was measured on the upper piston and the radial pressure was measured in three points by small pistons in contact with outer force transducers. After termination of the test the specimen was sliced and the density distribution in axial direction determined.

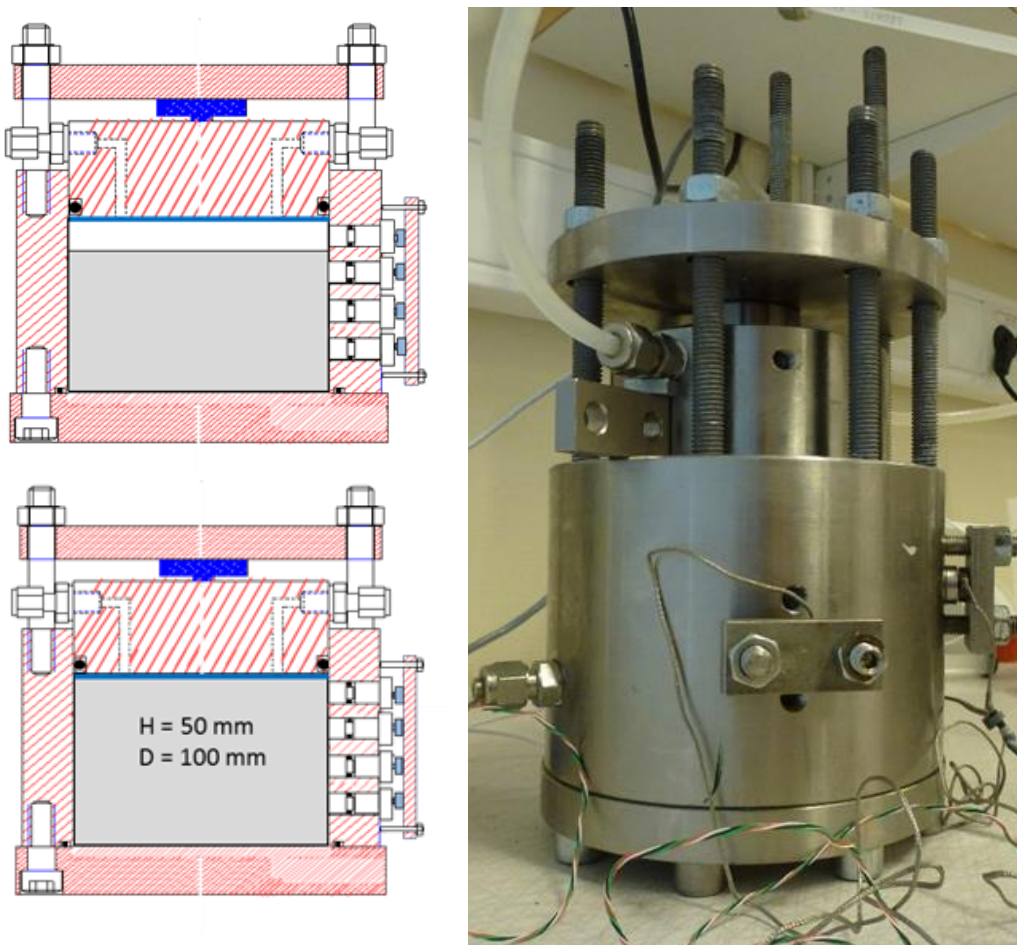


Figure 2: Set-up and a picture of one axial swelling test (HR-A). Water is supplied from a filter placed above the specimen. Radial swelling pressure measured 15 mm, 30 mm and 45 mm from the bottom of the test cell.

Table 2 shows the data for the test. In Figure 3 the distribution of ρ_d measured after termination of the test is shown. The results are shown with comparable test results from the basic series.

Table 2: Basic data of the test.

Test	Initial w (%)	Initial ρ_d (kg/m^3)	Constant diameter (mm)	Initial height (mm)	Final height (mm)	Swelling $\rho_{di}/\rho_{df}-1$ (%)
HR-A1	23.7	1 666	100	40	50	32

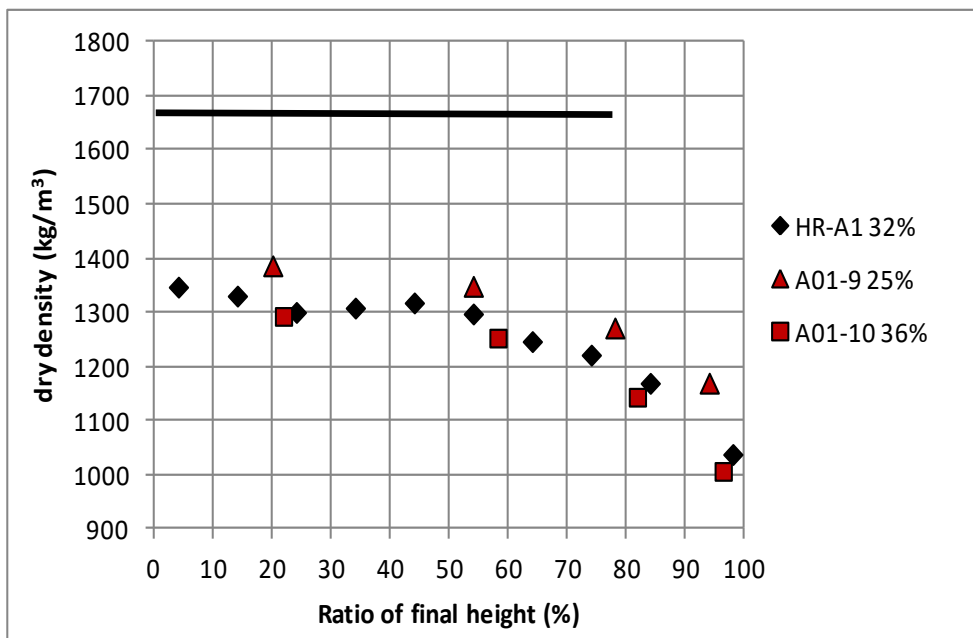


Figure 3: Distribution of measured dry density over specimen height, from bottom end surface and the initial dry density. Results from HR-A1 are shown together with results from the basic series.

The evolution of the swelling pressure is shown in Figure 4.

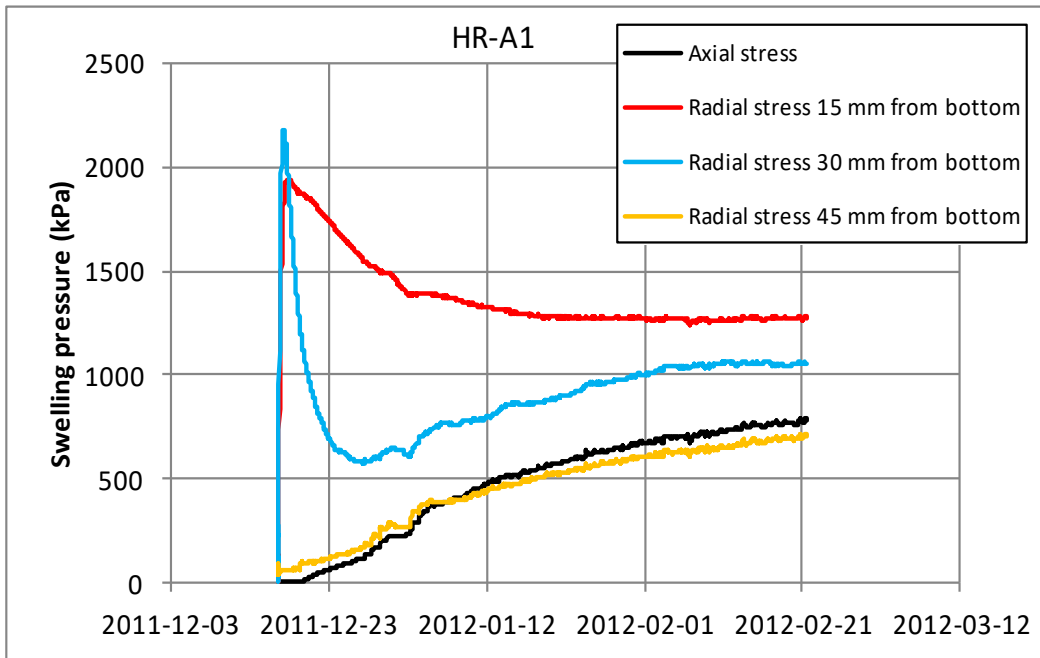


Figure 4: Time evolution of the swelling pressure from test HR-A1.

The density distribution shows that the specimen has homogenised very well with an overall decrease in dry density from 1666kg/m^3 to at most 1350kg/m^3 . The homogenisation is not complete since there is a remaining density gradient from about 1320kg/m^3 to about 1120kg/m^3 at the upper half of the specimen. The relative density distribution agrees well with the results from the basic test series (A01-9 and A01-10).

The stress evolution shows that the radial stress along the initial specimen height increases very fast in the beginning directly after water inlet but is then reduced due to the decrease in density with time. The upper radial stress above the initial specimen height and the axial stress increase slowly with time and end at lower stresses. The final stresses correspond well to the measured density distribution.

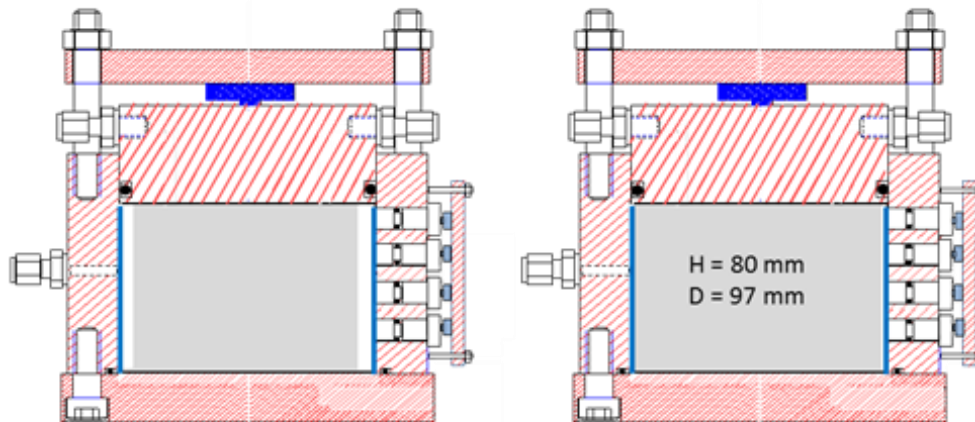


Figure 5: Set-up used for the radial outward swelling tests (HR-Ro). Water is supplied from a radial filter between the surrounding steel ring and the specimen. Axial swelling pressure is measured on the top lid and radial swelling pressure is measured 15 mm, 30 mm, 45 mm and 60 mm from the bottom of the test cell.

Table 3 shows the data for the test. In Figure 6 the distribution of ρ_d measured after termination of the test is shown. The results are shown with comparable tests from the basic series.

Table 3: Basic data of the test.

Test	Initial w (%)	Initial ρ_d (kg/m ³)	Constant height (mm)	Initial diameter (mm)	Final diameter (mm)	Swelling $\rho_{di}/\rho_{df}-1$ (%)
HR-Ro1	23.7	1666	80	81	96.8	42

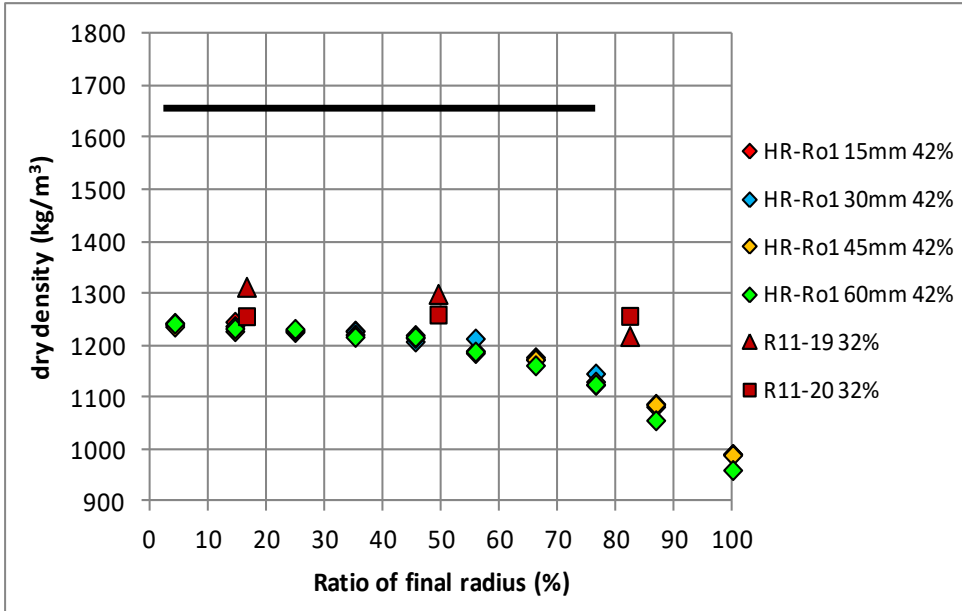


Figure 6: Distribution of measured dry density over the radius and the initial dry density. Result from HR-Ro1 is shown with results from the basic series; R11-19 and R11-20.

The evolution of the swelling pressure is shown in Figure 7.

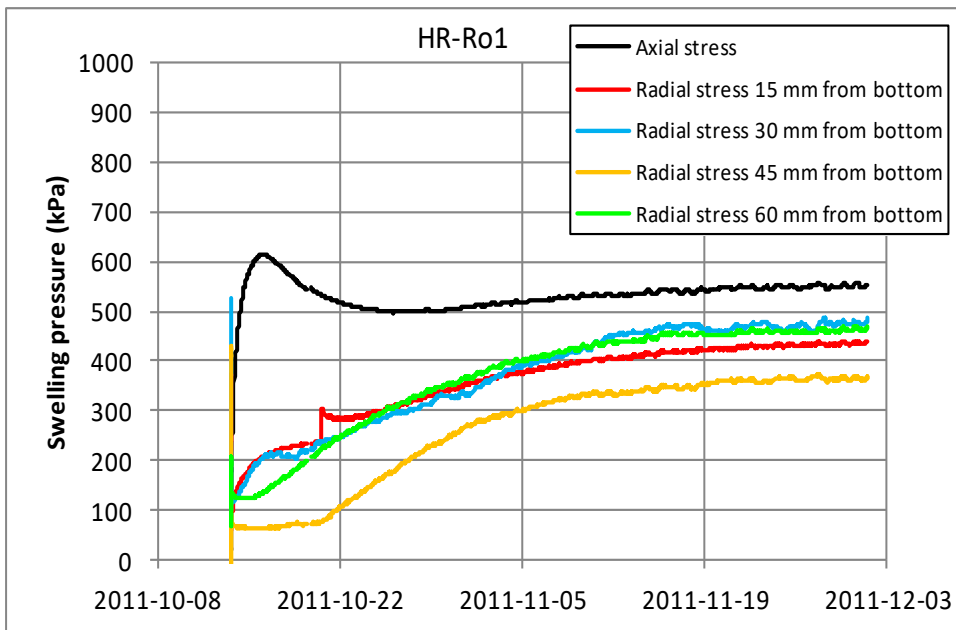


Figure 7: Time evolution of the swelling pressure from test HR-Ro1.

Figure 6 shows that the swelling and homogenisation is very good also in radial direction with an overall decrease in density from 1666kg/m^3 to less than 1250kg/m^3 . Just as for the axial swelling there is a remaining inhomogeneity outside about half the final radius with decreasing density down to slightly lower than 1000kg/m^3 . The density distribution was measured for four different slices and the results are very similar. The comparing results from the basic test series show better homogenisation, which is judged to mainly be caused by the larger swelling in the HR test.

As opposed to the axial swelling the measured axial pressure in the radial test is higher than the measured radial pressures, which is logical since there is no axial swelling. The radial pressures are as expected very similar with slight exception 45 mm from the bottom.

2.2 Swelling pressure - dry density relation

The following analyses are based on the fundamental swelling tests on MX-80 shown in Table 1. It is important to note that the swelling pressure in the test cells was determined as measured force on a piston placed axially or radially in contact with the specimen. The final values were measured after completed swelling and equilibrium when no or only small changes in pressure with time were seen. The water in equilibrium with the specimens was in the earlier part of the project stagnant water with a pressure of less than 5 kPa while in the later part of the project higher water pressure in combination with water circulation was used in order to get rid of air bubbles.

An important question is if the average stress and corresponding average density represent the conditions of the buffer also after swelling and homogenisation, i.e. to what extent the conditions agree with existing models of swelling pressure. The average stress $P_{average}$ is then calculated from the axial stress P_{axial} and radial stresses P_{radial} according to Equation 2.

$$P_{average} = (P_{axial} + 2 \cdot P_{radial})/3 \quad (2)$$

In Figure 8 the results from the fundamental swelling tests on MX-80 in the basic and the HR-series show that the average stresses after swelling and homogenisation agree well or are slightly higher compared to the model of MX-80 presented by Börgesson et al [10] when plotted with the corresponding average dry density. In Figure 8 an additional model of MX-80 is also shown, a model presented by Åkesson et al [11] and based on laboratory results from Karnland et al [7]. Compared to this model the measured swelling pressures are lower. The test results represent swelling mainly between 0 and 50% but also with a few tests between 90 and 110%. Test R11-21 is put in brackets since it deviated from the other tests both regarding swelling pressure and density distribution.

In Figure 8 the markers (circle, diamond) denote the test series (basic-series, HR series) and the colours (red, orange, blue) denote the type of swelling (axial, radial

outward, radial inward).

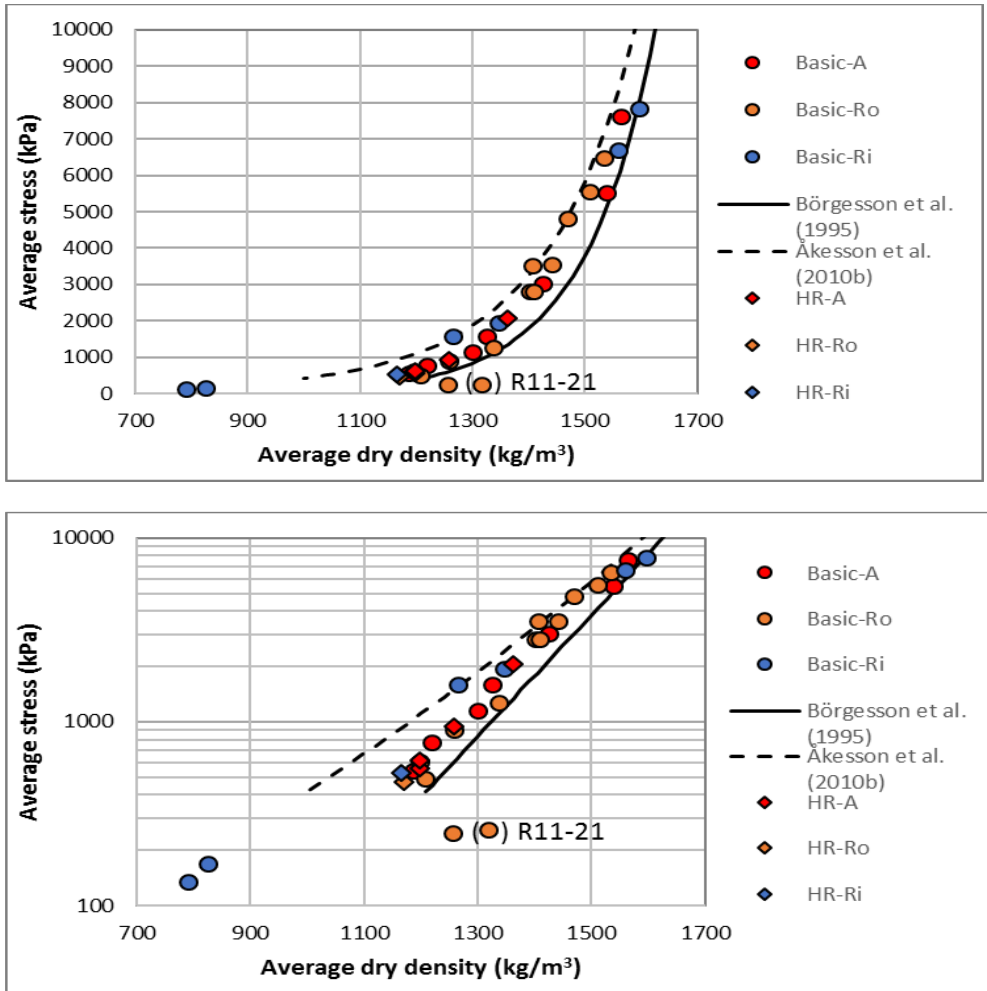


Figure 8: Average stress versus average dry density from almost all tests (i.e. according to Table 1) in the basic- and HR-series on MX-80. The results are plotted both with linear (upper) and logarithmic (lower) y-axis. The markers (circle, diamond) denote the test series (basic, HR) and the colors (red, orange, blue) denote the type of swelling (axial, radial outward, radial inward).

In Figure 8 it can be observed that the average stresses of MX-80 plotted as a function of the average dry densities after swelling and homogenisation show some scatter but is limited to values between the two models shown.

In Figure 9 the test results from the HR-series are shown again and in this plot the differences in stresses and densities in each test are marked with bars. The results correspond well with the solid line when conditions representing the highest dry density and highest measured stress from the tests are considered (i.e. the upper right corner of the square formed by the two bars given for each test) while conditions representing the lowest dry density and the lowest measured stress from each test are located far to the left of the solid line (lower left corner of the square formed by the bars given). This is caused by that different parts of the specimens are subjected to different stress paths, i.e. where the former conditions correspond to swelling at unloading the latter correspond to consolidation at loading. The dependence of stress paths has been seen earlier in oedometer tests where the density at equilibrium is higher when resulting from unloading, i.e. swelling from a higher stress state, compared to the density resulting from loading, i.e. consolidation from a lower stress state. However, while a specimen in an oedometer test mainly is exposed to either loading or unloading a specimen exposed to large swelling into an open void, as in the actual project, is exposed to both unloading and loading.

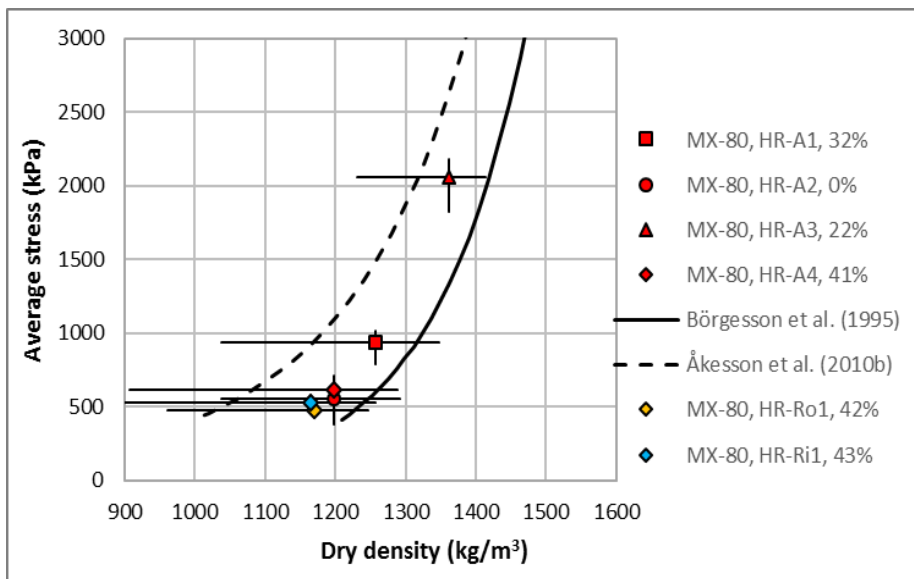


Figure 9: Results from all HR-tests of MX-80. The colors denote the type of swelling, the markers the size of the swelling and the bars show the maximum stresses and dry densities measured in each test. Two models of MX-80 are also shown.

The test results could be further studied by considering measured stresses and dry densities determined at specific positions in the test. In Figure 10, the radially measured stresses at different levels after axial swelling in the HR-series are plotted as a function of the dry density measured at the corresponding levels. Results from four tests on MX-80 with axial swelling in the HR-series are shown. In addition to the previous used models the results from the HR-series are plotted together with test results from previous studies on MX-80 and constant volume tests in the lower range of stresses (Karnland et al [12], Börgesson et al [10]).

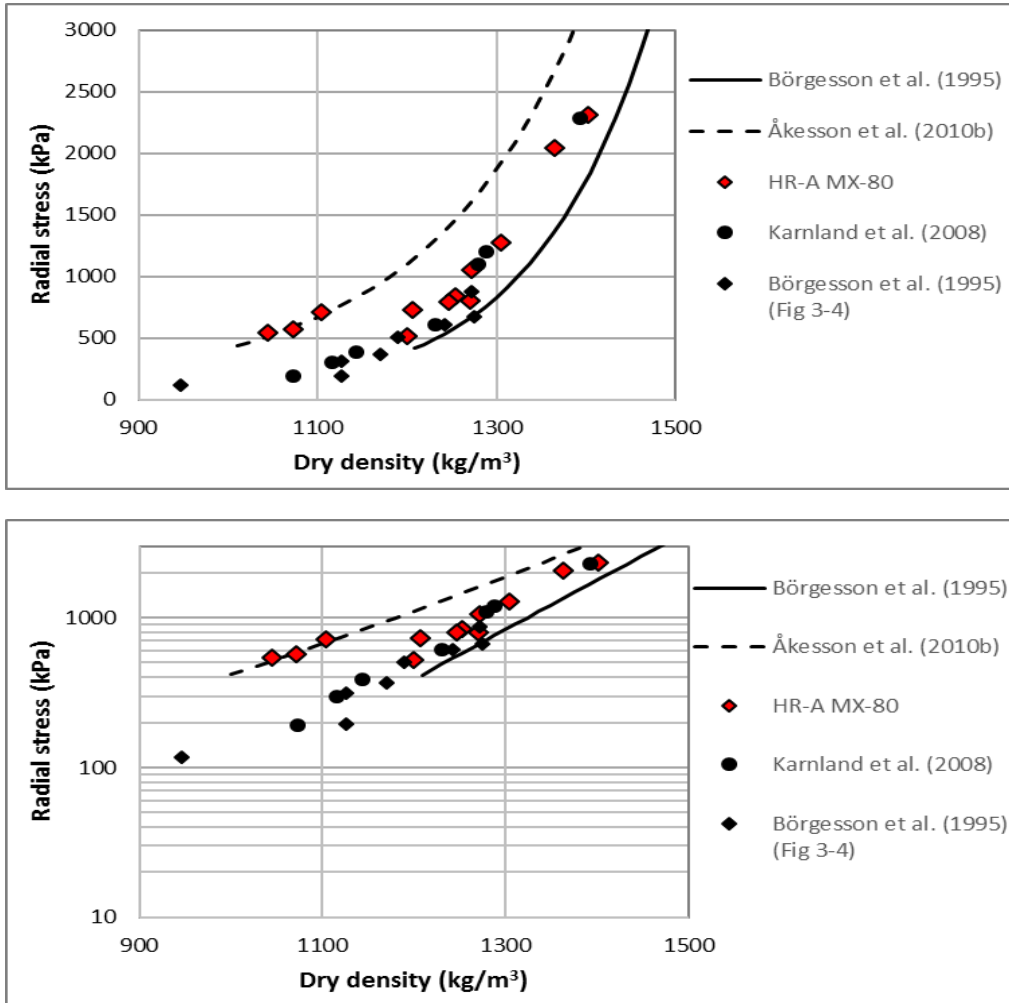


Figure 10: Radially measured stresses from tests on MX-80 in the HR-A series, i.e. axial swelling in the HR-series. The results are plotted as a function of dry density both with linear (upper) and logarithmic (lower) y-axis. Results from other studies on MX-80 are also plotted.

Most of the measured results on MX-80 from the HR-series correspond to the previous measurements and the solid line in Figure 10. However, the three red diamonds with marker lines located at the upper dotted line clearly deviate from the other measurements and all three are measurements from the uppermost position of three HR-specimens of MX-80, where the largest swelling has taken place. Thus, the deviating and somewhat extreme stress path of these three specimens seems to have influenced the final condition.

3. Measurement of friction between bentonite and other surfaces

The main reason for the remaining inhomogeneities after swelling is friction both against the confinement and in the bentonite itself. In order to investigate the friction between bentonite and outer surfaces a number of friction test series have been performed. In these test series the specimens were saturated with a minimum of swelling in a swelling pressure device consisting of a confining ring, pistons and plates. After completed saturation the friction tests were run by displacing the bentonite in relation to the confining ring, which had an inner surface prepared in different ways. The tested surfaces were either smooth steel surfaces, steel surfaces with machined grooves, a plastic filter surface or a surface of acrylic plastic. The results are presented as an interpreted friction angle as a function of measured swelling pressure. In these series mainly MX-80 specimens were used (18 tests) but two tests were also run on Calcigel.

The tests were carried out in the device shown in Figure 11. The swelling pressure device consists of a steel ring surrounding the specimen having filters on both sides. The inner surface of the ring can be prepared in different ways for example with or without lubrication. Two pistons are placed vertically, in the axial direction, above and below the specimen. A radial piston is placed in a hole through the steel ring for measurement of the radial pressure.

The bottom and top plates are bolted together to keep the volume constant. Three load cells are used for measurements of swelling pressure, two in the vertical direction and one in the radial direction. Each load cell is placed between a fixed plate and a movable piston where the small deformation required by the load cell is admitted. At shearing a third load cell and a deformation transducer are installed for measuring the force and deformation in the axial direction.

Cylindrical specimens were prepared by compaction of powder to a prescribed density. The specimens had a diameter of 50 mm and a height of 20 mm.

The tests consisted of two phases; the water saturation and the shearing phase. The entire test was done at constant volume conditions. The saturation started by mounting the specimen in the swelling pressure device and applying de-ionized water to the filters after air evacuation of the filters and tubes. When only small change in measured swelling pressure was noticed, the friction phase started.

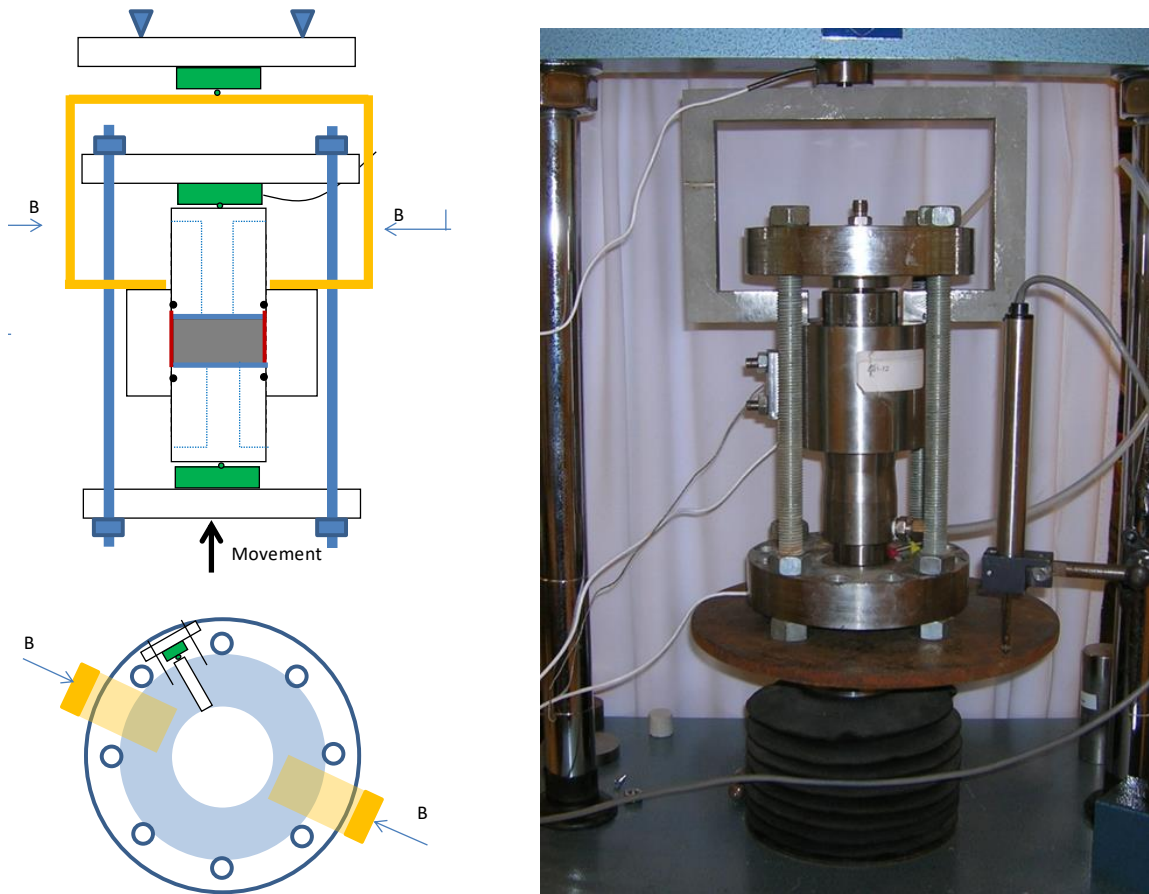


Figure 11: Set-up used for the study of friction between the bentonite buffer and other surfaces.

During the shearing phase the swelling pressure device was placed in a load frame (Figure 11) where the ring was fixed while the specimen was moved upwards with a constant rate, i.e. the specimen was pushed upwards through the ring. During this shearing phase the required force to keep the ring in place as well as the deformation and swelling pressure were measured. The specimen had free access to water during both the saturation and the subsequent friction phase. After shearing the bentonite specimen was dismantled and the distribution of water content and density over the specimen height were determined.

The friction angle was evaluated from Equation 3 where F is the measured force from the upper load cell, A_s is the radial surface area of the specimen, P_r is the radial stress perpendicular to the ring, and δ is the friction angle between the ring and the bentonite specimen.

$$F = A_s \cdot P_r \cdot \tan(\delta) \quad (3)$$

Examples of results on MX-80 are shown in Figure 12. The results in Figure 12 are from tests made in cylinders with different surfaces, smooth as well as grooved. The results show that, the friction angle evaluated at peak strength between the bentonite and the surfaces that had grooves corresponds well to the model of the bentonite internal friction angle presented by Åkesson et al [11]. The peak values when other surfaces were used yield lower friction angles. The largest difference between the peak and residual values are seen in the tests with grooves and at low swelling pressure.

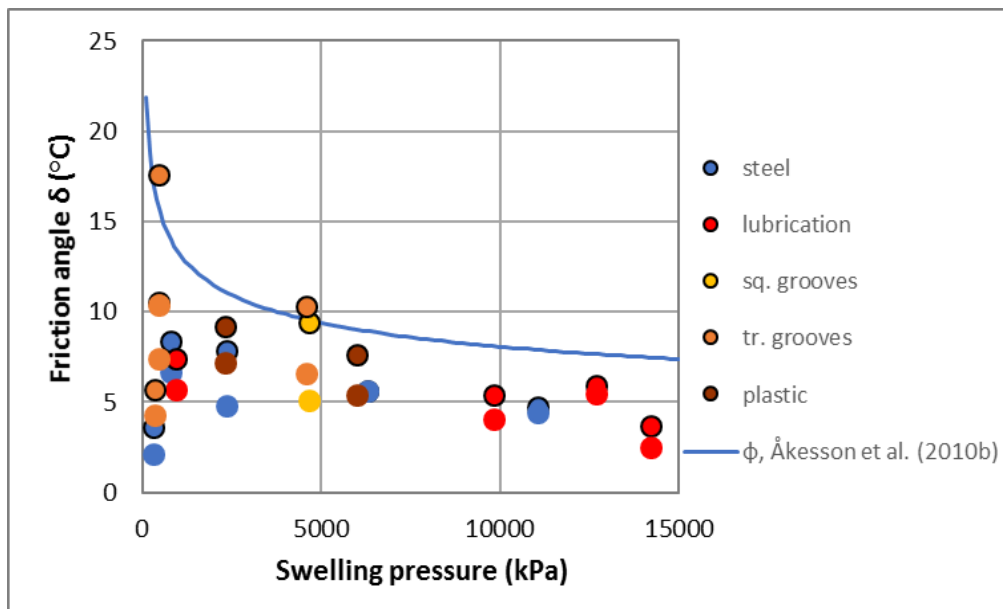


Figure 12: Friction angle as a function of swelling pressure from tests on MX-80 in the series with friction tests. The swelling pressure was measured radially. Marker lines around the symbols represent peak values and no marker lines represent residual values

The results can also be plotted as the measured shear stress as a function of the dry density, which is shown in Figure 13. In this diagram the line represents half of the maximum deviatoric stress, evaluated from a model presented by Børgesson et al [10], which is a measure of the shear strength. The results show that the main part of the evaluated peak stresses follows the model and the residual values are lower. In one of the tests on MX-80 where triangular grooves were used (light brown circles) the dry density determined after the test was uncertain and too low compared to the measured swelling pressure (see Table 5-8, Dueck et al [3]). This yields that in spite of that the results from this test fit well into Figure 12 they deviate in Figure 13 and are put in brackets.

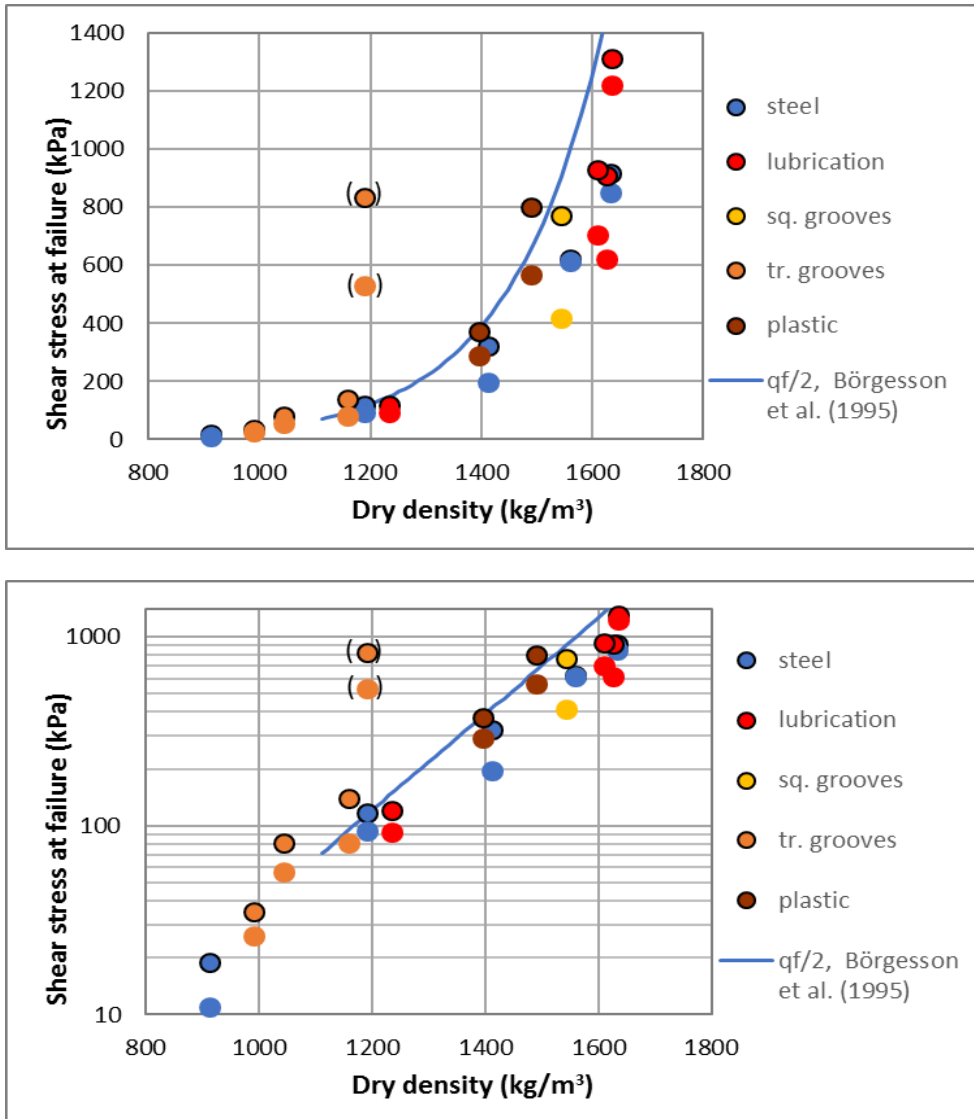


Figure 13: Shear strength as a function of dry density from the friction tests on specimens of MX-80. The values in brackets represent a test where the density was uncertain. Marker lines around the symbols represent peak values and no marker lines represent residual values. The results are plotted both with a linear y-axis and a logarithmic y-axis.

4. Homogenisation in long tubes

Swelling, compression and homogenisation of bentonite are studied by measuring the resulting density gradient of two bentonites in contact with each other in long tubes with very different initial densities of the bentonites. Ten tubes having similar designs and content are used for these tests. The length of the tubes are 10 times the diameter or 250 - 350 mm and 25 - 35 mm respectively. The lower half of each tube is filled with highly compacted bentonite and the upper half is filled with bentonite pellets. Water is added from the upper end, i.e. above the pellets. Swelling pressure is measured in some of the tubes by measuring radial and axial stresses exerted on pistons in the same way as in the HR tests. By using very different test durations the distribution of density and the evolution of swelling pressure can be studied as a function of time. One test has been finished after 2 years while nine are still ongoing.

The purpose of this test type is to study:

- the effect of friction for limiting homogenisation,
- the influence of time on the remaining density gradients after completed swelling and compression.

The result can also be used to evaluate how the so called “transition zones” in tunnels can be used to downshift the swelling pressure against e.g. a plug. One of the tests has been modelled and is further described by Börgesson et al [6].

A general sketch of the set-up used in this series is shown in Figure 14. The initial density of the highly compacted MX-80 bentonite in the lower part of the tube is about $\rho_d=1534\text{kg/m}^3$ and of the MX-80 pellets in the upper half of the tube about $\rho_d=882\text{kg/m}^3$. The expected void ratio/swelling pressure distribution after completed homogenisation is also illustrated. The length of the tubes was designed so that the initial densities of the pellets and the blocks would be kept at the ends of the tube. The tube walls contained milled grooves to increase the friction between the bentonite and the tube.

Four different varieties of the tube were manufactured with the main difference being the features of the inner wall and the dimensions of the tube. Square shaped grooves, triangular shaped grooves and a smooth inner wall were used. The different types of grooves are shown with greater details with the photos in Figure 15. Two different dimensions of tubes were used and while nine had the diameter 25 mm (and height 250 mm) one had the diameter 35 mm (and height 350 mm). Figure 16 shows a photo of 5 of the tubes after start. See Dueck et al [4] for further description.

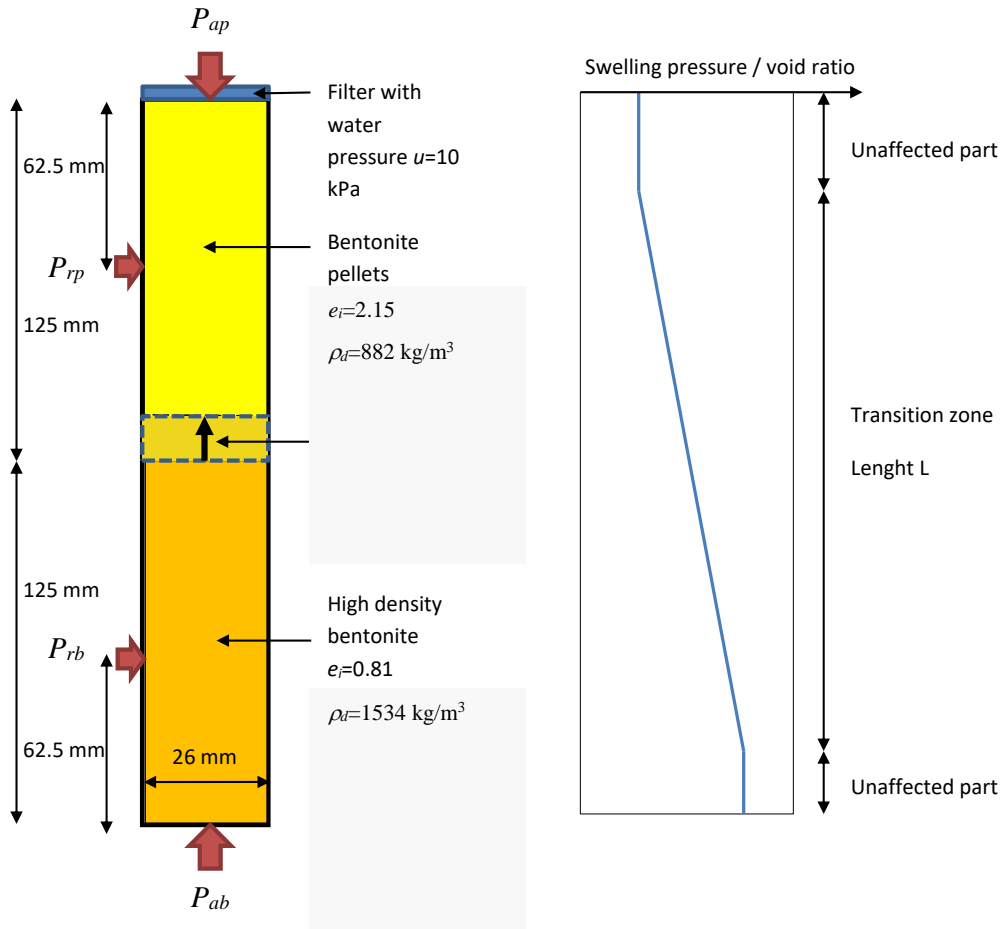


Figure 14: Illustration of the test, the transition zone and the expected swelling pressure and void ratio distribution after completed swelling. Red arrows mark pressure transducers.

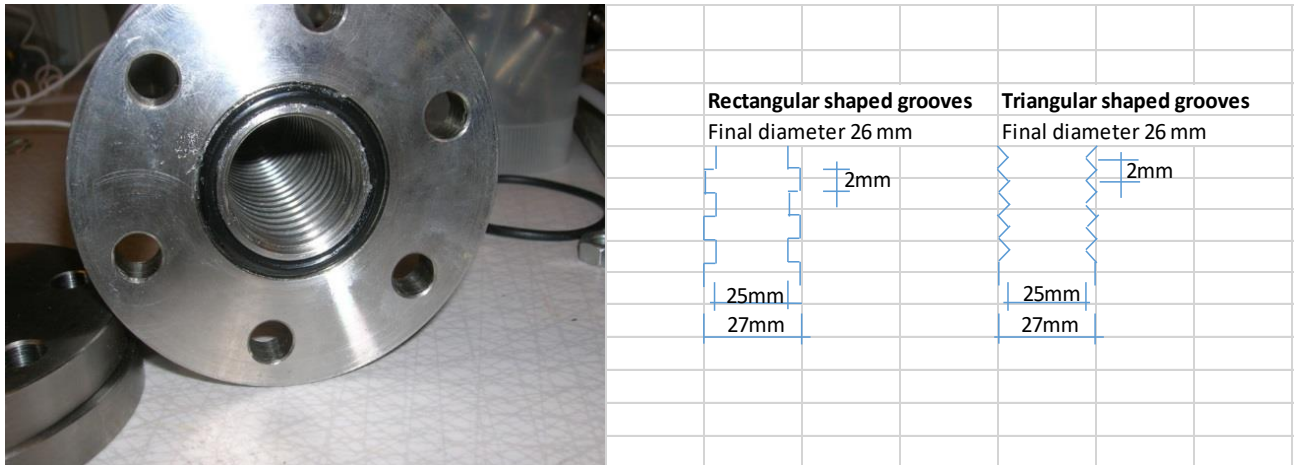


Figure 15: Photo and description of the geometry of the grooves.

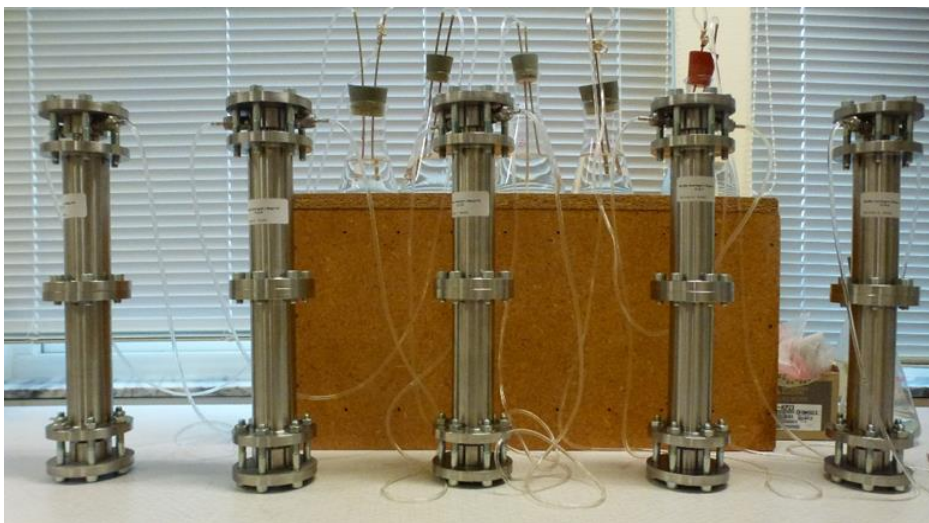


Figure 16: Photo of the non-instrumented tests FLR6 - FLR10 each attached to tubes used for water circulation.

The test started by adding a solution of 2-50 mM NaCl to the upper drainage, see Figure 16. The water was initially added by use of vacuum but after the initial phase a peristaltic pump was attached to the system to be used for the regular water circulation. After the planned testing period the tubes will be dismantled and the distribution of water content and density will be determined after slicing the specimen in thin radial slices for determining the axial density distribution.

The first dismantling was done after 2 years of test FLR5 and the second and third

dismantling are planned to be made after 4 and 8 years, respectively. Swelling pressure is measured in four (FLR1-FLR4) of the ten set-ups but not FLR5. The evolution of swelling pressure during the first two years, measured in test FLR2, which is similar to the one used for FLR5, is shown in Figure 17. The results of the sampling and measurement of dry density are shown in Figure 18.

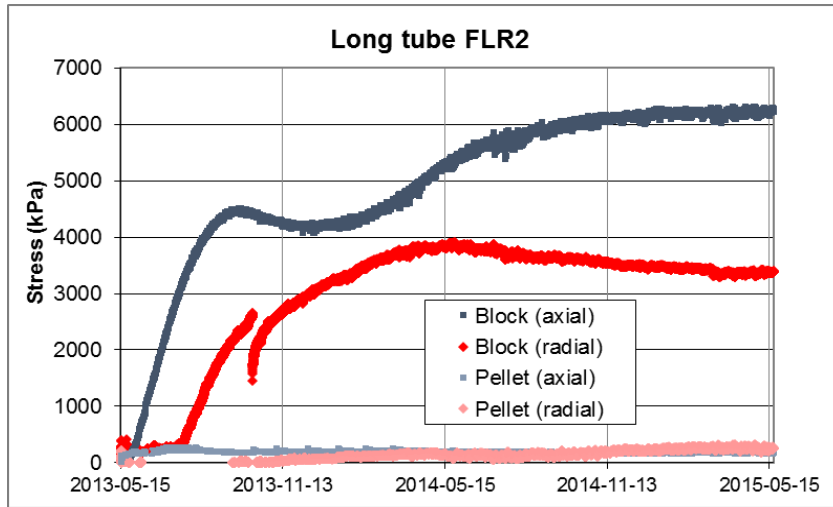


Figure 17: Swelling pressure measured during the test period of FLR5 but measured on the equivalent set-up of FLR2. The measurements have continued but the results after 2 years correspond to the time when test FLR5 was terminated. The location of the transducers is shown in Figure 14.

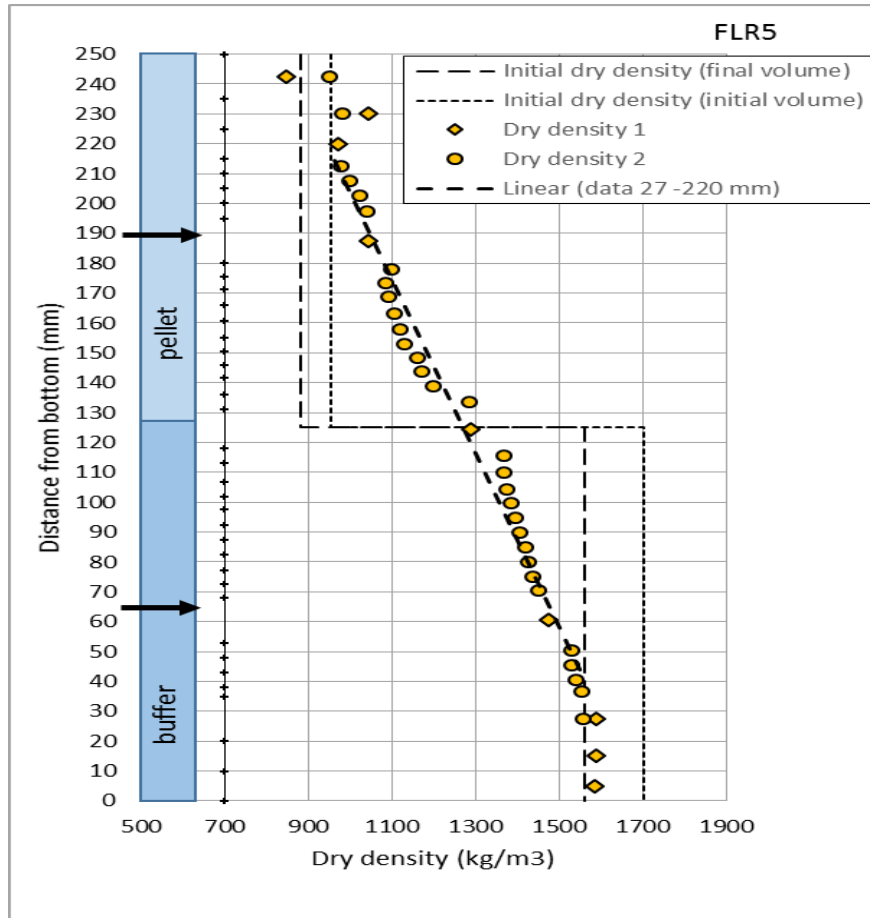


Figure 18: Distribution of measured dry density of test FLR5 after 2 years homogenisation. A best fit line for final dry densities between 27 mm and 220 mm is also shown.

Figure 19 shows the relation between the measured swelling pressure and the dry density at the measuring points

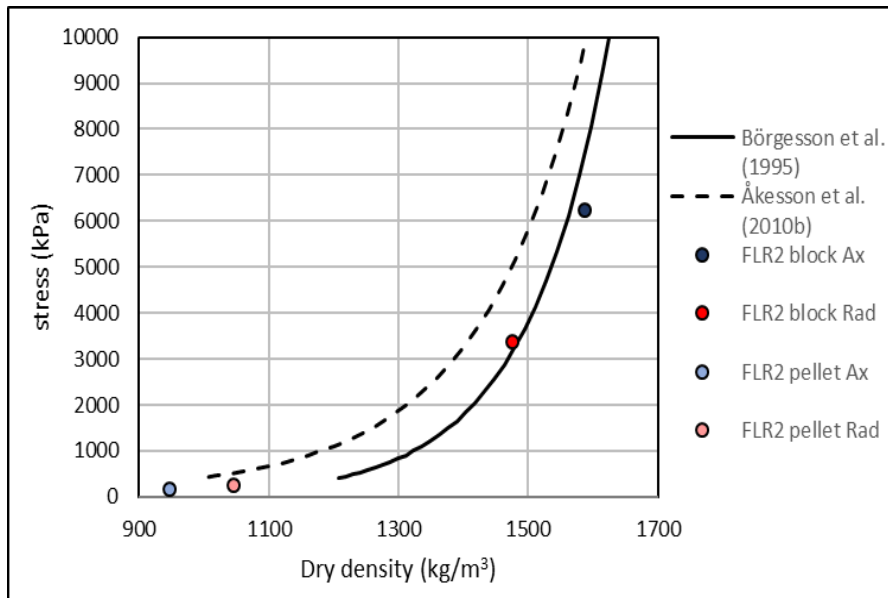


Figure 19: Swelling pressure measured in test FLR2 plotted for corresponding measured dry densities in test FLR5 together with the two swelling pressure models.

The swelling pressure measurements (Figure 17) show that at termination of the test, the axial swelling pressure at the bottom of the tube is as expected highest (6.2MPa), while the radial swelling pressure measured at the lower quarter of the tube is only about half of that (3.4MPa). The axial and radial swelling pressures at the upper pellet section are much lower (180kPa and 250kPa respectively). The swelling pressures seem to have stabilized after two years, which indicates that the homogenisation regarding pore pressure equalization is completed.

The density distribution (Figure 18) shows a remarkably linear density drop from the initial dry density of the block section to the initial density of the pellet section along the length of about 19cm, which was also predicted at the design of the equipment. There is obviously a transition zone that can be evaluated from the friction between the bentonite and the surrounding confinement in this type of geometry. Modelling of this case is shown in another article (Börjesson et al [6]).

5. Homogenisation after loss of bentonite - the self-healing tests

Two tests for simulating homogenisation of irregular cavities in a bentonite buffer of MX-80 have been performed. The two tests, SH1 and SH2, had the same boundary conditions and consisted of a block of MX-80 bentonite and they both started in December 2012. The non-instrumented SH2 was finished and dismantled after 17 months, in May 2014, and the instrumented SH1 was finished and dismantled after 33 months, in September 2015. One of the tests has been modelled and is further described in another article (Börgesson et al [6]). In this article the instrumented test SH1 will be described. More detailed information about SH1 can also be found in Dueck et al [4]. Results from SH2 were presented in Dueck et al [3].

The geometry of the set-up used for SH1 is shown with photos in Figure 20 and a sketch in Figure 21. The containment is a very stiff cylinder with the inner diameter 300 mm and the height 100 mm. An inner cylinder with the outer diameter 100 mm is included in the center mainly with the purpose to measure the swelling pressure and RH inside the bentonite block and to reduce the time for saturation and homogenisation. A stiff filter is mounted to the inside of the outer ring with the purpose to provide water to the bentonite from the radial surface. In each bentonite block two cavities were cut out in two diametrical positions in order to simulate loss of material. In the set-up of SH1 nine transducers for measuring swelling pressure and two for measuring suction were included.



Figure 20: Photos of the device and the bentonite block used for SH1. One of the cavities can be seen.

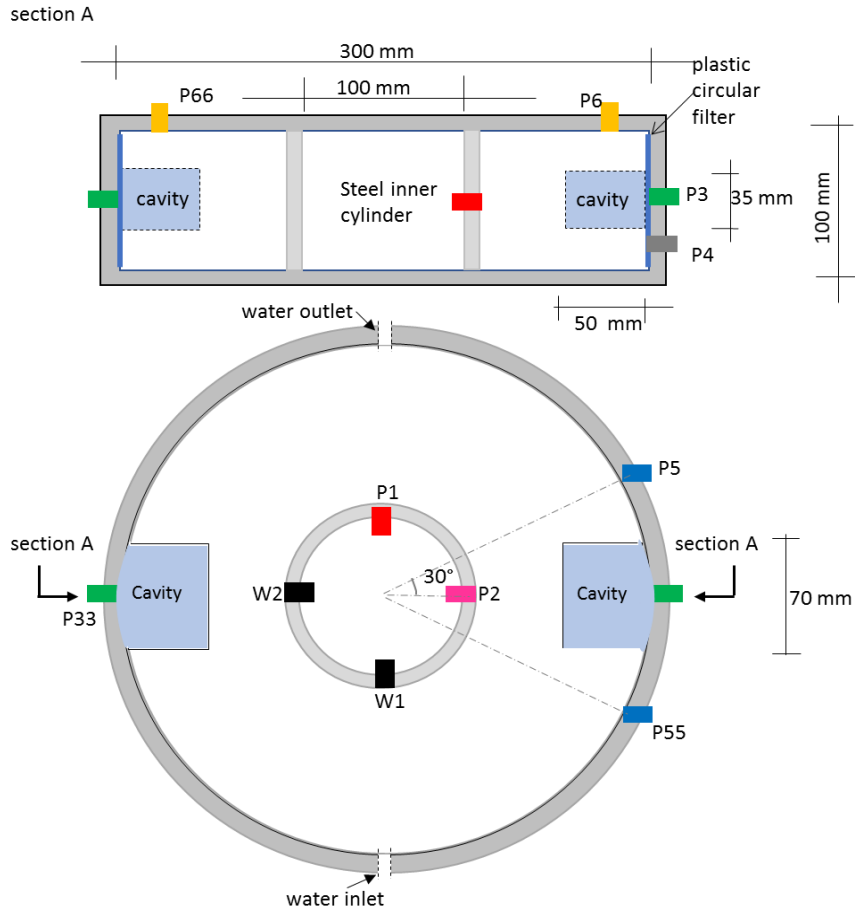


Figure 21: A sketch showing the positions of the sensors used in test SH1. The locations of the cavities and the water inlet and outlet are also shown.

Powder of MX-80 was mixed with de-ionized water to get a water content of 24% in order to reach a high initial degree of saturation after compaction. Aiming at a dry density of approximately 1660 kg/m^3 a compaction pressure of 40-60MPa was used for the uniaxial compacted cylinder block. The block was machined with a rotating lathe to the following dimensions: height =100 mm, outer diameter =298.7 mm and inner diameter =100.0 mm. There was thus a small gap of 0.65 mm between the block and the outer ring and virtually no gap at the inner ring and at the lids. Cavities were cut in two diametrical positions and the dimensions (height x length x depth) of the cavities in SH1 were $35 \times 70 \times 50 \text{ mm}^3$.

The properties of the bentonite block are shown in Table 4.

Table 4: Properties of installed bentonite

Properties including the small radial gaps but excluding the two cavities	Density	Particle density	Water density	Water content	Dry density	Void ratio	Degree of saturation
	ρ	ρ_s	ρ_w	w	ρ_d	e	S_r
	kg/m ³	kg/m ³	kg/m ³	%	kg/m ³		%
Initial conditions	2009	2780	1000	24.2	1618	0.72	94

Water was filled through the inlet pipe and air let out through the outlet pipe. Regular water flushing through the filter was made for de-airing purpose. After one hour approximately 94% of the available empty space mainly consisting of filter, gaps and cavities, was filled with water. 24 hours after the start approximately 97% of the available volume was filled.

Swelling pressure was measured in nine points in a similar way as described for the HR tests. seven of them were located in the outer ring and two in the inner ring (Figure 21). The results from the swelling pressure measurements in test SH1 are presented in Figure 22.

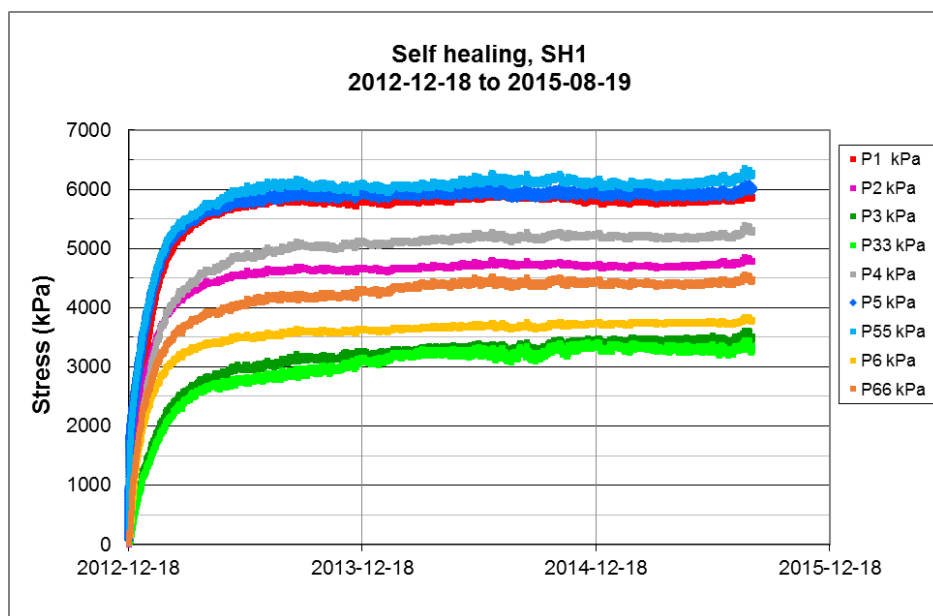


Figure 22: Evolution of swelling pressure from the transducers installed in test SH1. The locations of the sensors are shown in Figure 21.

Measurement of the water potential ψ , was made to follow the water saturation evolution of the bentonite in positions furthest away from the water source (sensors W1 and W2 located in the inner ring as shown in Figure 21). The measurements were made by thermocouple psychrometers, which evaluate the water potential by the Dew Point method (DP) and the Psychrometric method (P). Figure 23 shows the results. The sensor W1 stopped working after 7.5 months. The sensor W2 showed decreasing water potential until 16.5 months after start and after that no values were measured indicating water saturation. After some time though a low constant value was measured with the sensor W2. At the control after dismantling the sensor did not function properly. However, at the dismantling water was observed inside the casings surrounding the sensors W1 and W2, which also confirms that the block was completely water saturated.

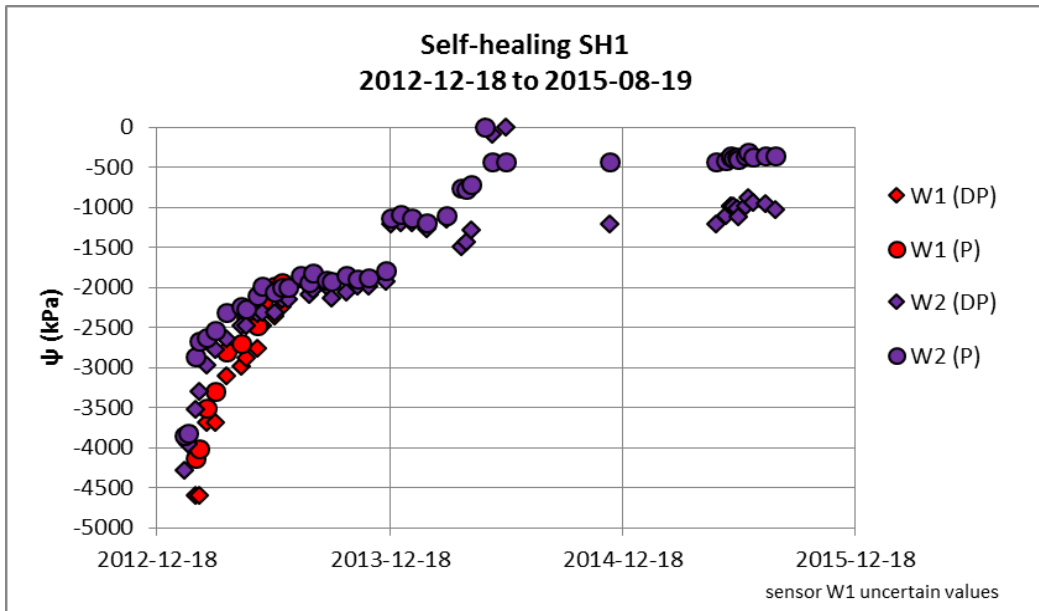


Figure 23: Evolution of water potential (suction) measured with thermocouple psychrometers installed in test SH1. The evaluation was made by both the dew point method (DP) and the psychrometer method (P). The labels show the number of the sensor (W1, W2) and the evaluation method (DP, P). The locations of the sensors are shown in Figure 21.

The test was terminated on 2015-08-19 and five days before termination the applied water pressure of 100kPa was lowered to zero. The dismantling started with lifting the lid and removing the bottom from the cylinder ring and then marking the planned sampling on the uncovered bentonite surfaces. The dismantling continued by free-drilling and removing the inner steel cylinder and dividing the bentonite cylinder into two half circles by sawing radially. Figure 24 shows photos taken during the dismantling.



Figure 24: Photos from the dismantling of SH1 just after lifting the lid.

The bentonite cylinder ring was divided into two half-cylinders during dismantling. One of the half-cylinders was directly used for the sampling and determination of water content and density distributions while the other one was sealed and stored for later analyses. Extensive sampling and measurement of the water content and the density was made. Figure 25 shows the sampling plan.

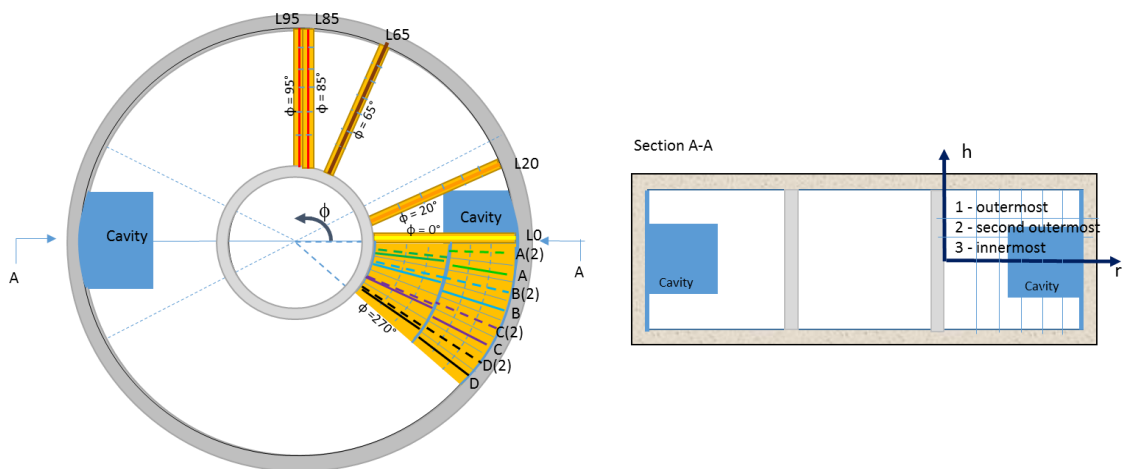


Figure 25: Plan view (to the left) which shows the sampling along lines at different angles from the middle of the cavity; 0° (yellow), 20° (orange), 65° (brown) and $85^\circ/95^\circ$ (red) and the sampling continuously within a sector along the dotted and solid lines (green, blue, purple and black). The section view (to the right) shows the different axial levels for the sampling; outermost, second outermost and innermost.

For further information on the sampling, see Dueck et al [4].

The measured distributions of dry density determined after dismantling of SH1 are shown in Figure 26. The dry densities of the samples from the sector were calculated from the measured bulk densities and water contents. In each diagram a small illustration of the location of the samples is given. The initial dry density of the block was approximately 1618kg/m^3 , see Table 4. The average final density based on the initial mass and the final volume of the device, i.e. with the cavities taken into account, was calculated to 1568kg/m^3 .

The distribution of dry density in different directions are shown as a function of the radial distance. The colours (red, brown, orange, yellow) show the results from the sampling lines (L85, L65, L20, L0) at the angles (85° , 65° , 20° , 0°) from the center of the initial cavity. Within the sector with continuous sampling the colours (green, blue, purple, black) show the sampling lines at the angles (6° , 17° , 28° , 39°) from the center of the initial cavity. Each subsector was further divided into two parts, marked with dotted and solid lines of each of the colours and from the center of the cavity the denomination of all sub-sectors are A(2), A(1), B(2), B(1), C(2), C(1), D(2), D(1).

The dry densities are logically lowest in the centre of the cavity (1400kg/m^3) and increases with increasing distance from the cavity.

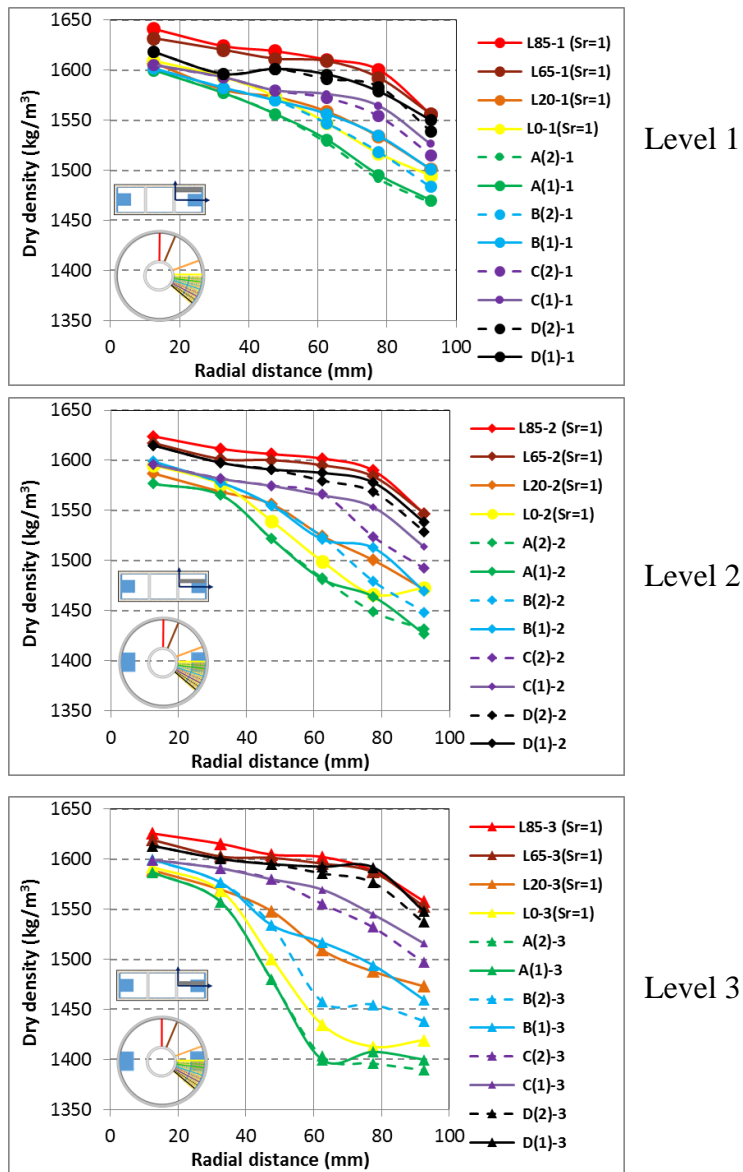


Figure 26: Distribution of dry density at the three levels (Figure 25) in different directions. The colours (red, brown, orange, yellow, green, blue, purple, black) show the angles (85°, 65°, 20°, 0°, -6°, -17°, -28°, -39°) to the center of the cavity. The values are calculated from measured water contents and 100% water saturation when the labels include (S_r=1).

6. Accuracies, uncertainties and limitations

Measurements and results often suffer from a scatter that could be caused by e.g. inaccurate devices and uncertain properties of the specimens. Such uncertainties put a limit to the usefulness of the results; for predictions and extrapolations. Below some examples from the actual laboratory test series are given.

The accuracy of the used sensors as load cells, pressure and deformation transducers are relatively high and since they are controlled regularly this will not limit the usefulness of the results. However, the radially measured stresses were done by use of small pistons and the measured stresses are thus representative for relatively small volumes. In addition, the small pistons measure towards a stiff material that requires a small deformation, which means that small irregularities may affect the results, but the swelling ability of the bentonite puts a limit to these errors. The axially measured stresses, on the other hand, were measured by use of a piston with larger cross section area, of the same size as the specimens. However, in tests involving radial swelling the measured axial stress did not represent a specific position but an average of the stresses at different radius.

The accuracy of the measured base variables after dismantling is rather high but the results from some tests showed large scatter in the calculated degree of saturation which usually is a measure of the uncertainty in the determination. However, in this study relatively large scatter in the degree of saturation was mainly observed in tests involving large density gradients over small distances. Since determination of degree of saturation requires two different samples that may differ in density and water content the scatter could be regarded as a measure of the difficulties to take representative specimens for determination of both water content and density from a small volume. Another variable where some uncertainty was noted was the initial density before swelling, especially when it was determined on trimmed specimens having somewhat uneven circumference. This influenced also the accuracy of the calculated swelling and densities in these tests.

7. Conclusions

The homogenisation properties of bentonite for buffer and backfill material have been investigated by a large number of very well controlled laboratory tests in different scales. The results provide valuable information about the behaviour and yield outstanding data that can be used for developing and checking homogenisation models and calibrating model parameters. Results from modelling of some of the tests are described in another article by Börgesson et al [6]. Ongoing laboratory tests and model development will additionally increase the knowledge and the skill to predict and understand different homogenisation scenarios.

A large number of fundamental very well controlled small-scale tests with simple geometries and swelling in radial or axial direction have been made. They show that homogenisation and healing properties of the investigated bentonites are extremely good but also that we after long time and with negligible changes in stress with time, still have considerable density differences that are dependent on the swelling

magnitude and initial density distribution. Some influence of time and applied water pressure was also found. The results show that the average stress and the average density after swelling agree well with the expected relations from constant volume swelling pressure tests. The results of the friction tests show that friction between bentonite and a raw steel surface, evaluated as a friction angle at peak stress, agree well with a model of the bentonite internal friction angle and that the corresponding residual friction angle and the friction angle when other smooth surfaces were used yielded lower values close to half the peak values.

Larger scale tests with more complicated geometries have been described and analysed. Two types of tests are shown. In one of the test types swelling and homogenisation in long tubes are studied with the purpose to investigate the effect of friction for limiting homogenisation and the influence of time on the remaining density gradients after completed swelling and compression. The tubes are 10 times longer than the diameter and while the lower half of each tube is filled with highly compacted MX-80 bentonite the upper half is filled with MX-80 pellets yielding a strong difference in initial density. One test has been finished after 2 years while nine are still ongoing. The final axial density distribution shows a remarkably linear density drop from the initial dry density of the block section to the initial density of the pellet section along about 75% of the total length, which was also predicted at the design of the equipment. The results can also be applied to evaluate to what extent the so called “transition zones” in tunnels can be used to downshift the swelling pressure against e.g. a plug.

The other test type simulates loss of bentonite in two medium scale laboratory tests, called Self-Healing tests (SH1 and SH2). A test device with the inner diameter 300 mm and the height 100 mm was used for the tests and a simulated canister with the outer diameter 100 mm was included in the centre. The water was provided to the bentonite from the outer radial surface. In each bentonite block two large cavities were cut out, in two diametrical positions, to simulate loss of material. After termination the bentonite was carefully sampled and the density of each sample determined yielding a final density distribution in three dimensions. The results show that the cavity has been very well healed by the swelling bentonite but also that the dry density in the centre of the former cavity is clearly lower (1400 kg/m^3) than the density at the unaffected parts (1640 kg/m^3).

ACKNOWLEDGEMENTS.

The study is funded by the Swedish Nuclear Fuel and Waste Management Company (SKB).

References

- [1] Dueck, A., Goudarzi, R. and Börgesson, L. (2011). Buffer homogenisation, status report. SKB TR-12-02. Svensk Kärnbränslehantering AB.
- [2] Dueck, A., Goudarzi, R. and Börgesson, L. (2014). Buffer homogenisation, status report 2. SKB TR-14-25. Svensk Kärnbränslehantering AB.
- [3] Dueck, A., Goudarzi, R. and Börgesson, L. (2016). Buffer homogenisation, status report 3. SKB TR-16-04. Svensk Kärnbränslehantering AB.
- [4] Dueck, A., Goudarzi, R. and Börgesson, L. (2017). Buffer homogenisation, status report 4. SKB TR-17-04. Svensk Kärnbränslehantering AB.
- [5] Dueck, A., Börgesson, L., Hernelind, J., Kristensson, O., Malmberg D. and Åkesson, M. (2018). Bentonite homogenisation. Laboratory study, model development and modelling of homogenisation processes. SKB TR-19-11. Svensk Kärnbränslehantering AB.
- [6] Börgesson, L., Hernelind, L. J. and Dueck, A. (2019). Bentonite homogenisation – modelling of homogenisation processes in buffer and backfill materials in repositories. *Journal of Earth Sciences and Geotechnical Engineering*, London. Special Issue on Disposal of Radioactive Waste Using Clay Barriers. 2019.
- [7] Karnland, O., Olsson, S. and Nilsson, U. (2006). Mineralogy and sealing properties of various bentonites and smectite-rich clay materials. SKB TR-06-30. Svensk Kärnbränslehantering AB.
- [8] Svensson, D., Dueck, A., Nilsson, U., Olsson, S., Sandén, T., Lydmark, S., Jägerwall, S., Pedersen, K. and Hansen, S. (2011). Alternative buffer material. Status of the ongoing laboratory investigation of reference materials and test package 1. SKB TR-11-06. Svensk Kärnbränslehantering AB.
- [9] Börgesson, L., Hernelind, J. And Åkesson, M. (2018). EBS TF - THM modelling. Homogenisation task. SKB P-18-05. Svensk Kärnbränslehantering AB.
- [10] Börgesson, L., Johannesson, L. E., Sandén, T. and Hernelind, J. (1995). Modelling of the physical behaviour of water saturated clay barriers. Laboratory tests, material models and finite element application. SKB TR-95-20. Svensk Kärnbränslehantering AB.
- [11] Åkesson, M., Börgesson, L. and Kristensson, O. (2010b). SR-site Data report, THM modelling of buffer, backfill and other system components. SKB TR-10-44. Svensk Kärnbränslehantering AB
- [12] Karnland, O., Nilsson, U., Weber, H. And Werson, P. (2008). Sealing ability of Wyoming bentonite pellets foreseen as buffer material - Laboratory results. *Physics and Chemistry of the Earth* 33, pages S472-S475. Elsevier Ltd.